Check for updates

Transboundary and Emerging Diseases

WILEY

RESEARCH ARTICLE OPEN ACCESS

First Report of Snakehead Rhabdovirus-Like *Novirhabdovirus* Associated With Acute Mortality in Multiple Outbreaks in Farmed Giant Snakehead (*Channa micropeltes*) in Thailand

Jidapa Yamkasem[1] | Natthakul Youngnoi[1] | Piyathip Setthawong[1] | Theeraporn Pulpipat[2] | Win Surachetpong[3] | Tuchakorn Lertwanakarn[1]

[1]Department of Physiology, Faculty of Veterinary Medicine, Kasetsart University, Bangkok, Thailand | [2]Department of Farm Resources and Production Medicine, Faculty of Veterinary Medicine, Kasetsart University, Kamphaeng Saen Campus, Nakhon Pathom 73140, Thailand | [3]Institute of Aquaculture, University of Stirling, Stirling, FK9 4LA, UK

Correspondence: Win Surachetpong (ws22@stir.ac.uk) | Tuchakorn Lertwanakarn (tuchakorn.l@ku.th)

Received: 1 April 2026 | **Revised:** 11 July 2026 | **Accepted:** 18 July 2026

Academic Editor: Linzhu Ren

Keywords: emerging virus | fish virology | *Novirhabdovirus* | pathogenesis | rhabdovirus

ABSTRACT

Snakehead rhabdovirus (SHRV) is a viral pathogen previously associated with mortality in snakehead fish (*Channa* spp.) and other closely related species. In this study, we report the detection of SHRV-like virus in giant snakehead (*C. micropeltes*) from multiple fish farms in Thailand, where acute disease outbreaks resulted in cumulative mortalities ranging from 7% to 90%. The affected fish showed clinical signs, including swimming near the water surface, anorexia, and skin discoloration. Histopathological examination revealed numerous eosinophilic intracytoplasmic inclusion bodies (ICIBs) in the spleen, anterior kidney, and posterior kidney. The virus was successfully isolated in E-11 cells, where it induced marked cytopathic effects (CPEs), including cell rounding, cytoplasmic vacuolization, and progressive monolayer destruction within 1–2 days post-inoculation (dpi). Transmission electron microscopy confirmed the presence of enveloped, bullet-shaped viral particles characteristic of the family *Rhabdoviridae*. Experimental challenge of naïve giant snakehead with the isolated virus reproduced the clinical signs observed in the field, resulted in 70% cumulative mortality within 4 days, and led to successful re-isolation of the virus from experimentally infected fish, which supports the pathogenic role of the virus in giant snakehead. Reverse-transcription polymerase chain reaction (RT-PCR) and sequence analysis demonstrated that the virus shared 79.70%–85.37% nucleotide identity with previously reported SHRV strains and placed the virus within the genus *Novirhabdovirus*, forming a cluster with SHRV and Carpione rhabdovirus (CAPRV). These findings provide evidence for the presence of a SHRV-like *Novirhabdovirus* associated with disease outbreaks in farmed giant snakehead in Thailand and highlight the need for further investigation into its epidemiology, pathogenesis, and transmission dynamics to support the development of effective disease prevention and control strategies.

This is an open access article under the terms of the Creative Commons Attribution License, which permits use, distribution and reproduction in any medium, provided the original work is properly cited.

Copyright © 2026 Jidapa Yamkasem et al. *Transboundary and Emerging Diseases* published by John Wiley & Sons Ltd.

1 | Introduction

Snakehead fish (*Channa* spp.) are air-breathing, carnivorous freshwater teleosts that are widely distributed across Asia and are becoming increasingly important for Asian aquaculture. Their ability to tolerate fluctuating environmental conditions, together with strong consumer demand for their firm and flavorful flesh, has facilitated the rapid expansion of snakehead farming in many Asian countries [1, 2]. Among these species, the giant snakehead (*C. micropeltes*) is of particular economic importance in Southeast Asia, including Thailand, Vietnam, Cambodia, Indonesia, and Malaysia, where it is farmed for both domestic and export markets [3–6]. To meet the growing production demand, giant snakehead farming has shifted toward more intensive pond-based systems, which are characterized by high stocking densities, limited water exchange, and suboptimal biosecurity. Although these practices help improve production volumes, they also create stress among fish, which reduces fish immunity and makes them more vulnerable to infectious diseases.

Among the various pathogens affecting snakehead species, bacterial pathogens, such as *Aeromonas hydrophila*, *A. veronii*, *Streptococcus iniae*, *Pseudomonas* spp., and *Brevundimonas vesicularis*, and parasitic infestations from, for example, *Trichodina* spp., *Ichthyobodo* spp., *Gyrodactylus* spp., and *Oodinium* spp., are frequently reported among farmed snakehead, and these associated diseases and loss of productivity cause substantial economic losses [7–9]. In contrast, viral diseases of snakehead fish remain poorly understood, and relatively little information is available regarding their diversity, epidemiology, and impact on aquaculture production.

Among the viruses reported in fish, members of the family Rhabdoviridae are recognized as some of the most important pathogens due to their association with severe disease outbreaks and substantial economic losses in aquaculture. This family includes several economically significant fish viruses, such as viral hemorrhagic septicemia virus (VHSV), infectious hematopoietic necrosis virus (IHNV), and spring viremia of carp virus (SVCV) [10]. These viruses primarily infect hematopoietic and endothelial tissues, leading to systemic infection characterized by hemorrhages, cell necrosis, and high mortality [10]. Within this family, snakehead rhabdovirus (SHRV), a member of the genus *Novirhabdovirus*, represents one of the few viral pathogens reported in striped snakehead (*C. striata*) and has subsequently been associated with disease outbreaks in China and India [11–13]. Infected fish typically show abnormal swimming behavior, lethargy, anorexia, and skin lesions that may progress to ulceration and acute mortality [14]. Mortality rates ranging from 70% to 90% have been reported during outbreaks, although confirmed infections have largely been restricted to *C. striata* and hybrid snakehead species [15, 16]. Despite the economic importance of giant snakehead (*C. micropeltes*), no molecular or virological evidence of SHRV infection has previously been documented in this species. Consequently, the emergence, pathological findings, and genetic characterization of SHRV in giant snakehead remain unknown. In this study, we describe the first detection of SHRV in farmed giant snakehead in Thailand during investigations of severe mortality outbreaks affecting multiple commercial fish farms. By integrating field investigations with histopathology, reverse-transcription polymerase chain reaction (RT-PCR), virus isolation, transmission electron microscopy, experimental challenge, and phylogenetic analysis, we investigated the pathological features and molecular identity of the causative agent. Our findings provide the first virological and molecular evidence of SHRV infection in this host species and indicate that SRHV should be considered in the diagnosis and management of disease in farmed giant snakehead.

2 | Materials and Methods

2.1 | Outbreak Investigation and Sample Collection

Between January and April 2025, acute mortality was reported in eight commercial giant snakehead farms located in Bangkok, Chachoengsao, and Phetchaburi provinces, Thailand. All the farms were stocked with juvenile giant snakehead fry (average initial weight: 3–15 g) sourced from nursery fish farms that had originally collected the fry from natural reservoirs. The fish were reared in earthen ponds without mechanical aeration. The management practices included a daily water exchange of approximately 10% using untreated water from adjacent public canals. Fish were fed once daily with minced marine forage fish at a rate of 3% of the estimated biomass. Stocking densities ranged from 12.5 to 15.6 fish/m^2, and the fish sizes varied from juveniles to market-sized adults (up to 3000 g). The affected populations were experiencing massive mortality, with cumulative losses reaching 90% within 2 weeks. During farm inspections, data on management practices, namely, fish sources, stocking density, feeding practices, and water flow, were obtained through interviews and recorded reviews. Water quality parameters (pH, ammonia, and nitrites) were measured using commercial kits (AquaCare, Bournemouth, UK) and a Pro20 multiparameter meter (YSI Inc., Yellow Springs, OH, USA).

Moribund fish were collected from each affected pond for diagnostic investigation. The fish were humanely euthanized via immersion in an overdose of eugenol solution (10 mL/L; Aquanes, Better Pharma, Lopburi, Thailand). External parasitological examinations were performed using wet-mount microscopy of skin mucus scrapings and gill filament biopsies. Aseptic necropsies were then conducted. Swabs from the anterior kidney were streaked onto tryptic soy agar (Difco, Le Pont de Claix, France) and incubated at 28°C for 18–24 h to allow bacterial growth. Representative tissues comprising the liver, spleen, anterior kidney, posterior kidney, brain, heart, intestines, and gills were collected for (i) histopathological analysis, (ii) RT-PCR, and (iii) virus isolation. All animal handling and sampling procedures were approved by the Institutional Animal Care and Use Committee (IACUC) of Kasetsart University (Protocol Number ACKU68-VET-058).

2.2 | Histopathology

During necropsy, tissue samples were collected from the gills, liver, spleen, anterior kidney, posterior kidney, brain, intestine, and heart of moribund giant snakehead from Farms 1, 2, 3, 4, 5, and 8. Fish from Farms 6 and 7 were excluded from histopathological analysis because the specimens arrived dead during transport. The tissue samples were fixed in 10% neutral buffered formalin for 24 h before being stored in 70% ethanol. The fixed

tbed, 2026, 1, Downloaded from https://onlinelibrary.wiley.com/doi/10.1155/tbed/9677946 by University Of Stirling, Wiley Online Library on [10/08/2026]. See the Terms and Conditions (https://onlinelibrary.wiley.com/terms-and-conditions) on Wiley Online Library for rules of use; OA articles are governed by the applicable Creative Commons License

tissues were then dehydrated through a graded ethanol series, cleared using xylene, and embedded in paraffin wax. Serial sections (4 μm thickness) were cut using a rotary microtome and stained with hematoxylin and eosin in line with standard protocols. The slides were examined under a light microscope, and representative images were captured using a virtual slide scanner (VS120, Olympus Corporation, Tokyo, Japan).

2.3 | Molecular Identification of the Virus

2.3.1 | RNA Extraction and RT

Posterior kidney tissues from the moribund fish were collected to screen for viral pathogens. The total RNA was extracted using the Genezol reagent (Geneaid, New Taipei City, Taiwan) in accordance with the manufacturer's instructions. Briefly, 30 mg of tissue was homogenized in 500 μL of Genezol reagent, mixed with chloroform, and incubated at room temperature. Following centrifugation at 12,000 × *g* for 15 min at 4°C, the aqueous phase was transferred to a new tube and mixed with an equal volume of isopropanol and then incubated at −20°C for 2 h to precipitate the RNA. The resulting pellet was washed twice with 75% ethanol, air-dried, and resuspended in pre-warmed diethyl pyrocarbonate-treated water. RNA purity and concentration were determined using a NanoDrop 2000/2000c Spectrophotometer (Thermo Fisher Scientific, Waltham, MA, USA). Complementary DNA (cDNA) was synthesized from 1 μg of total RNA in a 20 μL reaction using the ReverTra Ace qPCR RT Master Mix (Toyobo, Osaka, Japan). Each reaction contained 5× RT buffer, primer mix, RT enzyme mix, and nuclease-free water. RT was performed at 42°C for 60 min, followed by heat inactivation at 98°C for 5 min using a T100 touch-screen thermal cycler (Bio-Rad, Hercules, CA, USA).

2.3.2 | Detection of Rhabdoviruses by PCR

The initial screening for the Rhabdoviridae family was performed using conventional RT-PCR with primers that target the conserved block III region of the RNA-dependent RNA polymerase (*L*) gene [12]. Each 25 μL PCR reaction contained 0.6 μM of each forward and reverse primer, OneTaq DNA Polymerase (New England Biolabs, Ipswich, MA, USA), 200 ng of cDNA template, and nuclease-free water. Amplification comprised initial denaturation at 95°C for 2 min, followed by 35 cycles of 94°C for 30 s, 60°C for 45 s, and 72°C for 1 min, with a final extension at 72°C for 5 min. The PCR products were separated by electrophoresis on a 1.5% agarose gel containing ViSafe Green Gel Stain (Vivantis, Selangor, Malaysia) and visualized using the ChemiDoc MP Imaging System (Bio-Rad, Hercules, CA, USA). An amplicon of 483 bp was considered positive for the virus in the Rhabdoviridae family. To exclude other World Organization for Animal Health (WOAH)-listed fish rhabdoviruses [17], additional RT-PCR assays were performed on cDNA prepared from pooled kidney samples from each farm. These assays include primers targeting the glycoprotein (*G*) gene of infectious IHNV [18] and the nucleoprotein (*N*) gene of VHSV [19], with expected amplicon sizes of 693 and 319 bp, respectively. Furthermore, a nested RT-PCR targeting the *G* gene of SVCV [20] was conducted, with expected product sizes of 616 and 714 bp (Table 1).

2.4 | Virus Isolation

Virus isolation was performed using the E-11 cell line, a clone derived from the *C. striata* SSN-1 cell line (obtained from the European Collection of Authenticated Cell Cultures, UK). The E-11 cells were maintained in Leibovitz's L-15 medium (Sigma–Aldrich, St. Louis, MO, USA) supplemented with 10% fetal

TABLE 1 | Primers and RT-PCR targets used in this study.

Virus/family	Primers sequence (5′–3′)	Gene	Technique	Amplicon size (bp)	References
Rhabdoviridae	F: AAAGGTCGGGG GTTTGGACTAATG	*L*	RT-PCR	483	John et al. [12]
	R: CCAGACATACTG ACACAGCCCTTC				
IHNV	F: AGAGATCCCTACACCAGAGAC	*G*	RT-PCR	693	Emmenegger et al. [18]
	R: GGTGGTGTTGTTTCCGTGCAA				
VHSV	F: GGGACAGGAATGACCATGAT	*N*	RT-PCR	319	Kim et al. [19]
	R: TCTGTCACCTTGATCCCCTCCAG				
SVCV	F: TCTTGGAGCCA AATAGCTCARRTC	*G*	Nested RT-PCR	616	Stone et al. [20]
	R2: AGATGGTATGGACCC CAATACATHACNCAY				
	R4: CTGGGGTTTCCNCC TCAAAGYTGY			714	

Abbreviations: IHNV, infectious hematopoietic necrosis virus; SVCV, spring viremia of carp virus; VHSV, viral hemorrhagic septicemia virus.

tbed, 2026, 1, Downloaded from https://onlinelibrary.wiley.com/doi/10.1155/tbed/9677946 by University Of Stirling, Wiley Online Library on [10/08/2026]. See the Terms and Conditions (https://onlinelibrary.wiley.com/terms-and-conditions) on Wiley Online Library for rules of use; OA articles are governed by the applicable Creative Commons License

bovine serum (FBS) (Gibco, Waltham, MA, USA) and antibiotics (200 U/mL penicillin, 0.2 mg/mL streptomycin, and 0.5 μg/mL amphotericin B; Sigma–Aldrich, St. Louis, MO, USA). The cultures were incubated at 25°C without CO_2 and passaged at a ratio of 1:2 every 5–7 days.

For virus isolation, posterior kidney tissues (~30 mg) from the healthy and moribund giant snakehead were aseptically homogenized in 1 mL of L-15 medium (Sigma–Aldrich, St. Louis, MO, USA). The homogenates were centrifuged at 10,000 × *g* for 15 min at 4°C, and the supernatants were filtered through 0.22 μm syringe filters (Millipore, Billerica, MA, USA) to remove any bacterial contaminants. The filtrated inocula were then added to the confluent E-11 cell monolayers and incubated for 1 h at 25°C, after which a maintenance medium (L-15 supplemented with 2% FBS) was added. The cultures were incubated at 25°C and examined daily for cytopathic effects (CPEs) using an inverted microscope (Olympus CKX53, Tokyo, Japan). Once an extensive CPE (>70%) was observed, both the cells and culture supernatants were harvested and centrifuged at 3000 × *g* for 15 min at 4°C to remove the cellular debris. The supernatants were collected and stored at −80°C for further analysis. To confirm the presence of SHRV, the total RNA was extracted from the culture pellet, and RT-PCR targeting the *L* gene of Rhabdoviridae was performed using the primers and amplification conditions described in Section 2.3.

2.5 | Transmission Electron Microscopy

The culture supernatants with the confirmed presence of SHRV obtained in Section 2.4 were reinoculated onto the E-11 cell monolayers. The infected cells were harvested 1-day post-inoculation (dpi) for ultrastructural examination. The cells were scraped from the culture flasks and centrifuged at 2000 × *g* for 5 min at 4°C. The cell pellets were washed once with 0.1 M phosphate-buffered saline (PBS) (pH 7.4), centrifuged again, and immediately fixed in 2.5% glutaraldehyde (Electron Microscopy Sciences, Hatfield, PA, USA) at 4°C overnight. Following primary fixation, the samples were washed three times with 0.1 M PBS and postfixed in 1% (v/v) osmium tetroxide for 1 h at 4°C. The specimens were then dehydrated through a graded acetone series and embedded in epoxy resin [21]. Ultrathin sections (1 μm) were prepared, mounted on copper grids, and stained with 5% uranyl acetate. The grids were examined using a HT7700 transmission electron microscope (Hitachi High-Technologies, Tokyo, Japan), which was operated at 80 kV. The viral particles were identified and imaged at the Scientific Equipment and Research Division at Kasetsart University in Bangkok, Thailand. The morphology and dimensions of the observed virions were compared with those of previously described rhabdoviruses isolated from snakehead fish and other teleosts [12, 22, 23].

2.6 | Phylogenetic Analysis

Partial nucleotide sequences of the *L* gene (483 bp) obtained from the SHRV isolates were subjected to phylogenetic analysis together with representative fish rhabdovirus sequences retrieved from the NCBI GenBank database. Following agarose gel electrophoresis, the target amplicons were excised and purified using the GenepHlow Gel/PCR Kit (Geneaid, New Taipei City, Taiwan). The purified PCR products were sequenced bidirectionally using the Sanger sequencing method (Macrogen Inc., Seoul, South Korea). The resulting sequence chromatograms were examined for quality, and consensus sequences were assembled using the Benchling platform (www.benchling.com). The consensus *L* gene sequences were analyzed using BLASTn (NCBI, Bethesda, MD, USA) to identify homologous sequences and establish a preliminary viral classification. Closely related *L* gene sequences from various piscine rhabdoviruses were retrieved from the GenBank for comparative analysis. Multiple sequence alignments were performed using the MAFFT algorithm implemented in the GenomeNet online platform (https://www.genome.jp/). Phylogenetic trees were initially constructed using the neighbor-joining method with 1000 bootstrap replications to assess the reliability of the tree topology. A maximum likelihood phylogenetic tree was subsequently reconstructed in MEGA version 12 (https://www.megasoftware.net/) following model selection analysis performed in MEGA, and the general time-reversible model with gamma-distributed rate variation among sites and a proportion of invariant sites (GTR + G+I) was selected as the best-fitting substation model based on the lowest Bayesian information criterion score [24]. The final dataset included representative members of the genus *Novirhabdovirus*, including SHRV, VHSV, IHNV, Carpione rhabdovirus (CAPRV), and Hirame rhabdovirus (HIRRV). To provide a broader evolutionary context within the family Rhabdoviridae, numerous fish rhabdoviruses, such as SVCV, Eel virus European, and other types of rhabdoviruses (i.e., Chandipura virus, rabies lyssavirus, Sonchus yellow net virus, apple rootstock virus A, potato yellow dwarf virus, and Arboretum virus) were included as outgroups.

2.7 | Experimental Viral Challenge in Healthy Giant Snakehead

Twenty-five healthy juvenile giant snakehead (mean body weight: 50 ± 1.2 g), obtained from a nursery farm in Samut Sakhon province, Thailand, were acclimated in 150 L glass tanks for 28 days. During the acclimation and experimental periods, water quality parameters, including temperature (28 ± 1°C), dissolved oxygen, pH, ammonia, and nitrite levels, were monitored daily. Prior to the challenge, five fish were randomly selected and screened by histopathological examination, microbiological culture, parasitological examination, and RT-PCR to confirm the absence of bacterial, parasitic, and rhabdovirus infections. All five fish tested negative in all assays. The remaining 20 fish were randomly assigned to either an experimental group ($n = 10$) or a control group ($n = 10$).

On the experimental day, fish were sedated in a 40 mg/L eugenol solution (Aquanes, Better Pharma, Lopburi, Thailand). Fish in the experimental group were given an intracelomic injection with 100 μL of culture supernatant derived from passage 2 rhabdovirus-positive E-11 cells. The viral inoculum originated from a rhabdovirus isolate recovered from a fish collected at Farm 4, the only farm in which no parasitic or bacterial coinfections were detected. Fish in the control group were injected with an equal volume of supernatant from normal E-11 cells via the same route, as described elsewhere [25]. Following inoculation, fish in both groups were monitored daily for clinical signs, behavioral abnormalities, and mortality for 14 days post-challenge (dpc). Posterior kidney samples were collected from moribund fish for (i) confirmation of rhabdovirus infection by RT-PCR, (ii) viral re-isolation

tbed, 2026, 1, Downloaded from https://onlinelibrary.wiley.com/doi/10.1155/tbed/9677946 by University Of Stirling, Wiley Online Library on [10/08/2026]. See the Terms and Conditions (https://onlinelibrary.wiley.com/terms-and-conditions) on Wiley Online Library for rules of use; OA articles are governed by the applicable Creative Commons License

through inoculation onto E-11 cell monolayers, and (iii) subpassage of the recovered virus in E-11 cells.

3 | Results

3.1 | Clinical Signs and Gross Pathology

We investigated mortality outbreaks across eight giant snakehead farms in Bangkok, Chachoengsao, and Phetchaburi provinces, Thailand, between January and April 2025 (Figure 1 and Table 2). The affected fish ranged from juveniles (3–15 g) to market-sized adults (>1 kg) (Figure 1A–C). Cumulative mortality among the farms varied substantially—from 7% to 90%—with the highest losses recorded in Farms 1, 2, and 4. The clinical signs of swimming near the water surface, lethargy, reduced appetite, and sudden death were most evident among the fish at the farms where acute mortality was experienced. Upon gross examination, multifocal skin ulcerations and occasional fin erosion were observed in the fish from Farms 1 and 2 (Figure 1D). In contrast, the fish from the remaining farms showed generalized skin discoloration or lacked obvious external lesions (Figure 1E). Internal examinations consistently revealed splenomegaly, pale and friable livers, and kidney enlargement (Figure 1F,G). External parasitological examination of the gills and skin mucus showed *Trichodina* spp. infestations in the fish from Farms 1 and 2; however, no ectoparasites were detected in the samples from the other farms. Bacteriological cultures of the anterior kidney samples yielded *Aeromonas* spp. in the fish from Farms 1, 2, 5, and 8, whereas the samples from the remaining farms showed no bacterial growth (Table 2).

3.2 | Rhabdovirus Detection and Histopathological Findings

Posterior kidney samples from 30 fish collected across the eight farms were tested for the presence of rhabdovirus using conventional RT-PCR targeting the *L* gene. Of the 30 fish examined, 16 (53.3%) tested positive, with at least one positive fish identified from each of the eight farms (Supporting Information 1: Table S1). Histopathological examination was performed on tissue samples collected from 20 fish originating from Farms 1, 2, 3, 4, 5, and 8 (Supporting Information 1: Table S1). Histopathological changes were primarily observed in the hepatic and hematopoietic tissues of affected fish (Figure 2), although the severity and distribution of lesions varied among fish and farms. In the liver, marked hepatocellular vacuolization was the most common finding and was observed in fish from Farms 1, 2, 4, 5, and 8 (Figure 2A,B; Supporting Information 1: Table S1). In the hematopoietic organs, the spleen and anterior kidney showed depletion of red blood cells, increased numbers of melanomacrophage centers, and numerous eosinophilic intracytoplasmic inclusion bodies (ICIBs) associated with cellular pyknosis (Figure 2C–F). Similarly, the posterior kidney of affected fish showed extensive eosinophilic ICIBs and numerous pyknotic cells within the interstitial tissue (Figure 2G,H), often accompanied by tissue necrosis in more severely affected fish. Collectively, these histopathological findings were indicative of viral infection and were observed in fish from all six farms (Supporting Information 1: Table S1). Examination of the gills revealed lamellar edema, basal congestion, and mild lymphocytic infiltration in affected fish (Supporting Information 2: Figure S1A), whereas mild vascular congestion was observed in the brain of some fish (Supporting Information 2: Figure S1B). No remarkable histopathological changes were observed in the intestine or heart (Supporting Information 2: Figure S1C, D). In addition to the lesions indicative of viral infection, multifocal granulomatous inflammation was found in the liver, spleen, anterior kidney, and posterior kidney of fish from Farms 1 and 2, where concurrent infections with *Aeromonas* spp. *and Trichodina* spp. were detected.

3.3 | Screening of Other Piscine Rhabdoviruses Using RT-PCR

Pooled posterior kidney samples from each farm were screened for other notifiable piscine rhabdoviruses listed by the WOAH

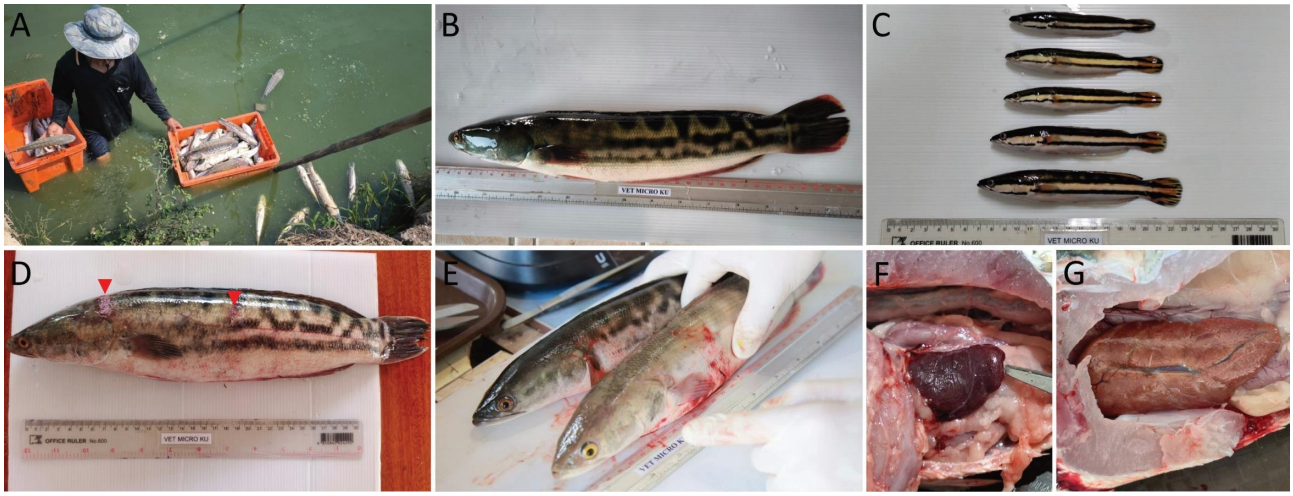

FIGURE 1 | Clinical signs and gross pathological findings in moribund giant snakehead during disease outbreaks across the central region of Thailand in January–April 2025. (A) Mass mortality in a commercial grow-out earthen pond. (B, C) Clinical presentation of affected adult and juvenile giant snakehead. (D) Severe multifocal cutaneous ulcerations with fin erosion (red arrowheads) in fish from Farms 1 and 2. (E) Moribund fish with generalized pale skin color (bottom fish). (F) Internal gross pathology showing splenomegaly with characteristic bulging edges. (G) Pale and friable liver indicating hepatic lipidosis or glycogen depletion.

tbed, 2026, 1, Downloaded from https://onlinelibrary.wiley.com/doi/10.1155/tbed/9677946 by University Of Stirling, Wiley Online Library on [10/08/2026]. See the Terms and Conditions (https://onlinelibrary.wiley.com/terms-and-conditions) on Wiley Online Library for rules of use; OA articles are governed by the applicable Creative Commons License

TABLE 2 | Summary of field investigations and diagnostic findings from eight giant snakehead farms in Thailand that experienced mortality outbreaks in January to April 2025.

Farm	Province	Collection date	Fish weight (g)	Cumulative mortality (%)	Clinical signs	Necropsy findings	Parasite screening	Bacterial screening
1	Phetchaburi	February 6, 2025	690–820	90	Swimming near the water surface, loss of appetite, and lethargy	Pale and sedimented gills, scale protrusion, and hemorrhagic skin ulcers. Splenomegaly with multifocal white nodules in the spleen, anterior kidney, and posterior kidney. Enlargement of the anterior kidney and posterior kidney.	*Trichodina* spp.	*Aeromonas* spp.
2	Phetchaburi	February 6, 2025	1200–1800	80–90	Swimming near the water surface, loss of appetite, and lethargy	Skin hemorrhaging, pale liver, and necrosis. Splenomegaly with multifocal white nodules in the spleen, anterior kidney, and posterior kidney. Enlargement of the anterior kidney and posterior kidney.	*Trichodina* spp.	*Aeromonas* spp.
3	Chachoengsao	February 12, 2025	370–540	10	Normal behavior	Mild petechiae. Pale gills and skin discoloration	ND	ND
4	Chachoengsao	February 12, 2025	300–1450	80–90	Swimming near the water surface, loss of appetite, and lethargy	Pale gills and skin discoloration	ND	ND
5	Bangkok	February 24, 2025	700–800	20	Swimming near the water surface, loss of appetite, and lethargy	Skin discoloration and ggpetechial hemorrhage	ND	*Aeromonas* spp.
6	Bangkok	April 4, 2025	3–5	15	Normal behavior	ND	ND	ND
7	Bangkok	April 4, 2025	8–15	15	Normal behavior	ND	ND	ND
8	Chachoengsao	April 18, 2025	1200–1800	7	Normal behavior	Cloudy eyes and skin discoloration	ND	*Aeromonas* spp.

Abbreviation: ND, not detected.

tbed, 2026, 1, Downloaded from https://onlinelibrary.wiley.com/doi/10.1155/tbed/9677946 by University Of Stirling, Wiley Online Library on [10/08/2026]. See the Terms and Conditions (https://onlinelibrary.wiley.com/terms-and-conditions) on Wiley Online Library for rules of use; OA articles are governed by the applicable Creative Commons License

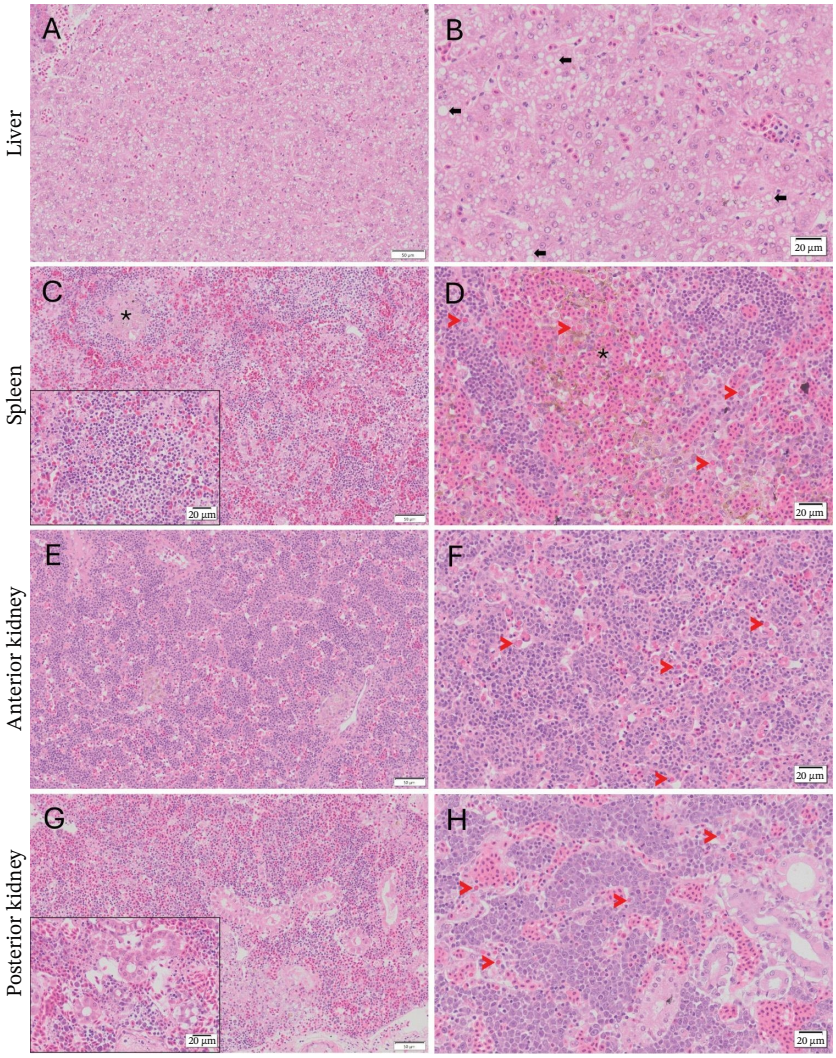

FIGURE 2 | Histopathological changes in the tissues of the moribund giant snakehead from Farm 4. (A, B) Liver sections showing marked glycogen depletion and prominent hepatocellular vacuolization (black arrows). (C, D) Spleen showing the severe depletion of mature erythrocytes, multiple and extensive cellular pyknosis (inset), increased formation of melanomacrophage centers (asterisks), and numerous eosinophilic intracytoplasmic inclusion bodies (ICIBs; red arrowheads). (E, F) Anterior kidney showing hematopoietic cell depletion and abundant eosinophilic ICIBs (red arrowheads). (G, H) Posterior kidney displaying extensive pyknotic cells within the interstitial tissue surrounding the renal tubules (inset) as well as numerous ICIBs (red arrowheads).

using conventional RT-PCR. RT-PCR assays targeting the *G* gene of IHNV, the *N* gene of VHSV, and the *G* gene of SVCV (nested PCR) were performed on cDNA prepared from the pooled tissues from each of the eight farms. No amplification was detected for IHNV, VHSV, or SVCV in any of the pooled samples from the eight farms (Figure 3A–C), thereby excluding these three rhabdoviruses as the causative agents of the observed disease. Results of SHRV detection at the individual fish level and subsequent virus isolation are presented in Section 3.4 and Table 3.

3.4 | Virus Isolation in E-11 Cell Culture

Posterior kidney homogenates from sampled fish were inoculated onto confluent monolayers of E-11 cells for viral isolation. Control E-11 (Figure 4A,B) and cells inoculated with rhabdovirus-negative tissue homogenates (Figure 4C,D) showed no remarkable changes throughout the 5-day observation period. In contrast, cells inoculated with rhabdovirus-positive posterior kidney samples exhibited marked CPEs, characterized by cell rounding and cytoplasmic vacuolization, as early as 1 dpi (Figure 4E). By 2 dpi, extensive CPE was observed, resulting in complete destruction of the E-11 cell monolayer (Figure 4F). Of the 30 outbreak-derived samples inoculated onto E-11 cells, 16 (53.3%) developed characteristic CPE during the observation period (Table 3). Further RT-PCR analysis of culture supernatants confirmed the presence of rhabdovirus RNA in 17 CPE-positive cultures (Table 3).

3.5 | Transmission Electron Microscope

Samples confirmed as rhabdovirus-positive by RT-PCR were propagated in E-11 cells, followed by ultrastructural characterization via transmission electron microscopy (Figure 5). Ultrathin sections of the infected cells revealed numerous enveloped viral particles distributed throughout the cytoplasm. The virions, which were observed both within the cytoplasm and at the cell

tbed, 2026, 1, Downloaded from https://onlinelibrary.wiley.com/doi/10.1155/tbed/9677946 by University Of Stirling, Wiley Online Library on [10/08/2026]. See the Terms and Conditions (https://onlinelibrary.wiley.com/terms-and-conditions) on Wiley Online Library for rules of use; OA articles are governed by the applicable Creative Commons License

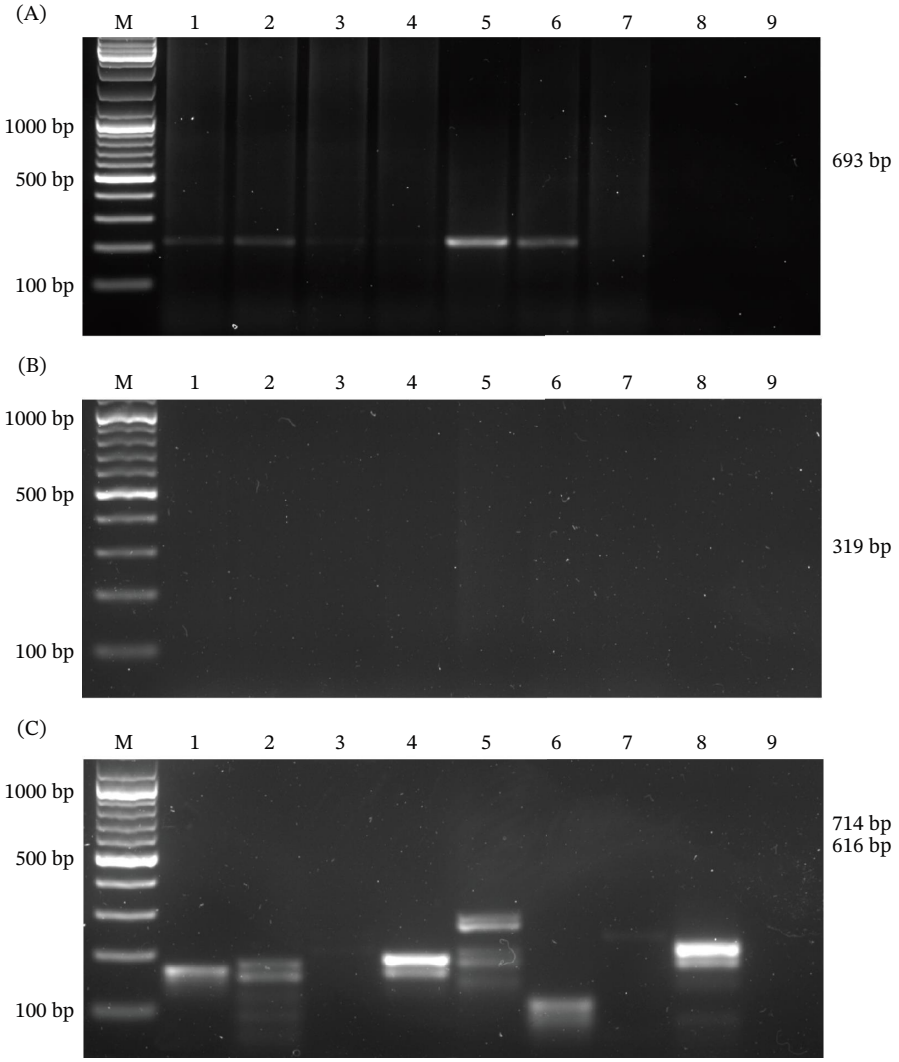

FIGURE 3 | Molecular screening of pooled posterior kidney samples from giant snakehead farms by conventional RT-PCR targeting. (A) The glycoprotein (*G*) gene of infectious hematopoietic necrosis virus (IHNV; 693 bp). (B) The nucleoprotein (*N*) gene of viral hemorrhagic septicemia virus (VHSV; 319 bp). (C) The glycoprotein (*G*) gene of spring viremia of carp virus (SVCV; 714 and 616 bp). Lane M, DNA molecular weight marker; lanes 1–8, pooled tissues from Farms 1–8, respectively; lane 9, no-template control.

membrane during budding, had the bullet-shaped morphology characteristics of members of the family *Rhabdoviridae*. The viral particles measured approximately 150–200 nm in length and 50–80 nm in width and contained an electron-dense core of variable size and electron density.

3.6 | Phylogenetic Analysis Based on the *L* Gene

Partial nucleotide sequences (436–458 bp) of the *L* gene were obtained from SHRV isolates from Farms 1 and 4 (five sequences; GenBank accession numbers PZ043849–PZ043853). BLASTn analysis showed that the SHRV from the giant snakehead shared a nucleotide identity of 84.86%–85.37% with 100% query coverage to a reference SHRV strain isolated from striped snakehead (*C. striata*) in Thailand (GenBank accession AF147498.1). In addition, the isolates showed 79.90%–80.19% nucleotide identity, with 92%–95% query coverage, to a SHRV strain reported from *C. striata* in India (GenBank accession MT459927.1). To determine the phylogenetic relationships of these isolates with representative members of the family Rhabdoviridae, the five *L* gene sequences were analyzed alongside 15 reference strains (Figure 6). Phylogenetic reconstruction placed the virus identified in this study within the genus *Novirhabdovirus*. The five isolates from this study clustered tightly together with strong bootstrap support (100%). Within this group, the three isolates recovered from Farm 4 (PZ043851, PZ043852, and PZ043853) formed a distinct subcluster supported by a bootstrap value of 98%, while the two isolates from Farm 1 (PZ043849 and PZ043850) grouped together with moderate bootstrap support (67%). The SHRV from the giant snakehead formed a strongly supported clade with previously reported SHRV strains from striped snakehead in Thailand (AF147498.1) and India (MT459927.1) with 100% bootstrap support. Together with CAPRV reference strains from Italy (LC630942.1) and China (PP050495.1), they constituted a well-supported SHRV–CAPRV cluster (100% bootstrap support). This cluster was clearly separated from other representative members of the genus *Novirhabdovirus*, including VHSV (Y18263.1), HIRRV (AF104985.2), and IHNV (L40883.1), with strong bootstrap support for all major nodes. Based on the phylogenetic relationship inferred from the partial *L* gene sequences, the virus identified in this study was

tbed, 2026, 1, Downloaded from https://onlinelibrary.wiley.com/doi/10.1155/tbed/9677946 by University Of Stirling, Wiley Online Library on [10/08/2026]. See the Terms and Conditions (https://onlinelibrary.wiley.com/terms-and-conditions) on Wiley Online Library for rules of use; OA articles are governed by the applicable Creative Commons License

TABLE 3 | Summary of virus isolation in E-11 cell culture and RT-PCR confirmation of rhabdovirus from giant snakehead collected from diseased outbreaks at eight farms in Thailand.

Farms	Province	Sample ID	E-11 CPE	Cell culture RT-PCR
1	Phetchaburi	Fish 1	+	+
		Fish 2	+	+
		Fish 3	−	+
		Fish 4	+	+
2	Phetchaburi	Fish 1	+	+
		Fish 2	−	−
		Fish 3	−	−
3	Chachoengsao	Fish 1	−	−
		Fish 2	+	+
		Fish 3	−	−
4	Chachoengsao	Fish 1	+	+
		Fish 2	+	+
		Fish 3	+	+
		Fish 4	+	+
		Fish 5	+	+
		Fish 6	+	+
5	Bangkok	Fish 1	+	+
6	Bangkok	Fish 1	+	+
		Fish 2	+	+
		Fish 3	−	−
		Fish 4	−	−
		Fish 5	−	−
7	Bangkok	Fish 1	−	−
		Fish 2	−	−
		Fish 3	+	+
		Fish 4	−	−
		Fish 5	−	−
8	Chachoengsao	Fish 1	−	−
		Fish 2	−	−
		Fish 3	+	+
Total			16/30 (53.3%)	17/30 (56.7%)

Note: +, positive for RT-PCR detection; −, negative for RT-PCR detection.

designated as an SHRV-like *Novirhabdovirus* isolates KU-SHRV-CM01 to KU-SHRV-CM05 (GenBank accession numbers PZ043849–PZ043853).

3.7 | SHRV-Like *Novirhabdovirus* Establishes Infection in Experimentally Challenged Giant Snakehead

The SHRV-like *Novirhabdovirus* isolate KU-SHRV-CM03 isolated from Farm 4 was selected and subsequently introduced to the naïve giant snakehead using intracelomic injection. By 2 dpc, experimentally infected fish showed clinical signs including lethargy, anorexia, abnormal swimming behavior, loss of balance, and skin decoloration. Mortality was first observed at 2 dpc and continued until 4 dpc, resulting in a cumulative mortality of 70% (7/10 fish). No additional mortality was recorded among the surviving fish during the remainder of the 14-day observation period. In contrast, no clinical signs or mortality were observed in the control group throughout the experiment (Figure 7A). The posterior kidney tissues collected from all experimentally challenged fish tested positive for rhabdovirus by RT-PCR, whereas all samples from the control fish tested negative (Figure 7B). The

tbed, 2026, 1, Downloaded from https://onlinelibrary.wiley.com/doi/10.1155/tbed/9677946 by University Of Stirling, Wiley Online Library on [10/08/2026]. See the Terms and Conditions (https://onlinelibrary.wiley.com/terms-and-conditions) on Wiley Online Library for rules of use; OA articles are governed by the applicable Creative Commons License

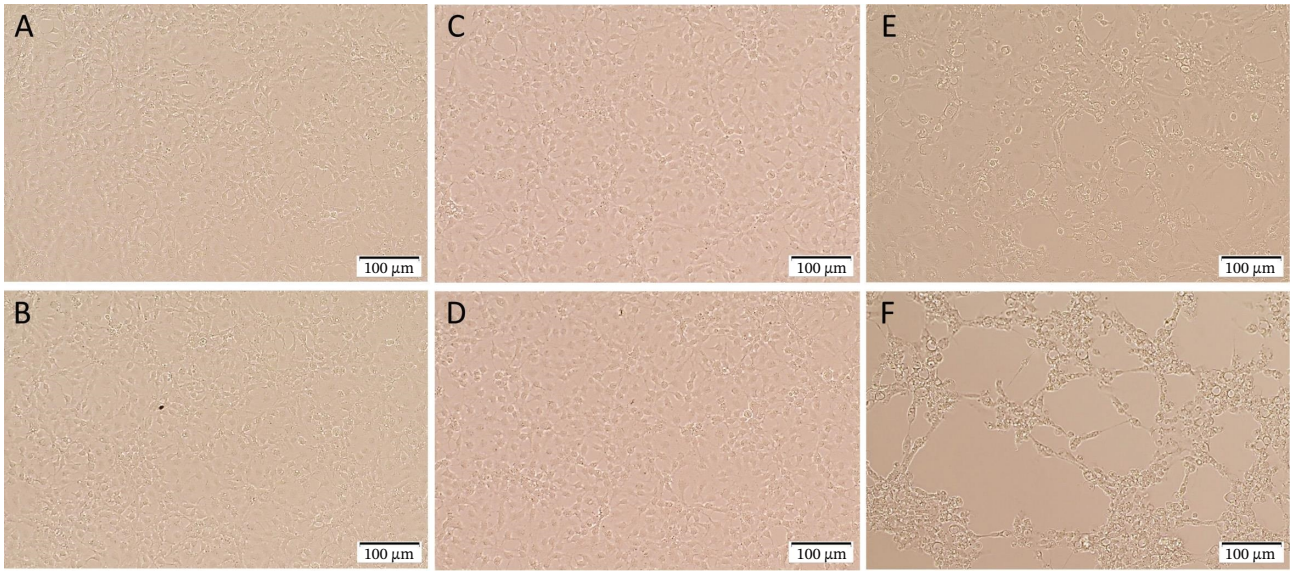

FIGURE 4 | Virus isolation and morphological investigations of E-11 cells inoculated with posterior kidney homogenates obtained from giant snakehead. (A, B) Uninfected control E-11 cells at 0 and 5 days post-inoculation (dpi), showing normal monolayer morphology throughout the observation period. (C, D) E-11 cells inoculated with posterior kidney homogenate from a rhabdovirus-negative giant snakehead at 0 and 5 dpi, showing no observable CPE. (E, F) E-11 cells inoculated with a rhabdovirus-positive posterior kidney homogenate, showing early CPE characterized by cell rounding and vacuolization at 17dpi, and extensive CPE resulting in the extensive destruction of the cell monolayer at 27dpi.

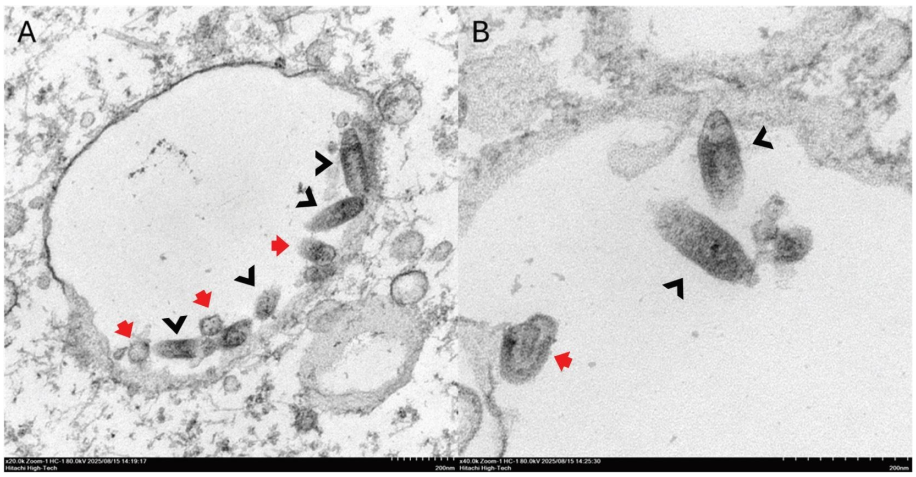

FIGURE 5 | Transmission electron micrographs of snakehead rhabdovirus-infected E-11 cells. (A) Ultrathin sections of E-11 cells harvested at 1-day post-inoculation (dpi) showing numerous bullet-shaped virions (black arrowheads) and budding viral particles (red arrows) distributed within the cytoplasm and at the cell membrane. The virions are enveloped and contain an electron-dense nucleocapsid core. (B) Higher magnification image of a representative virion exhibiting the characteristic bullet-shaped morphology consistent with members of the family Rhabdoviridae. Budding viral particles (red arrows) and mature virions (black arrowheads) are visible. Scale bar = 200 nm.

virus was successfully re-isolated in E-11 cells using posterior kidney homogenates from RT-PCR-positive fish. During the first passage (P1), a characteristic CPE was observed within 2 dpi, affecting more than 50% of the cell monolayer. Following sub-passage of the recovered virus (P2), the CPE developed more rapidly and extensively, affecting more than 80% of the cells within 1 dpi and progressing to extensive cell detachment and clumping by 2 dpi (Figure 7C). RT-PCR analysis of P2 culture supernatants confirmed the presence of the SHRV-like *Novirhabdovirus* in the infected cells.

4 | Discussion

SHRV, a member of the family Rhabdoviridae, has been widely reported in striped snakehead and hybrid snakehead species and is associated with disease outbreaks and substantial mortality in aquaculture systems across Asia [11–14, 26]. Despite the growing economic importance of giant snakehead in Southeast Asian aquaculture, viral pathogens affecting this species have been poorly studied. Our findings provide molecular, virological, ultrastructural, and experimental evidence supporting the occurrence of SHRV infection in the farmed giant snakehead. This finding not only identifies giant snakehead as a susceptible species to

tbed, 2026, 1, Downloaded from https://onlinelibrary.wiley.com/doi/10.1155/tbed/9677946 by University Of Stirling, Wiley Online Library on [10/08/2026]. See the Terms and Conditions (https://onlinelibrary.wiley.com/terms-and-conditions) on Wiley Online Library for rules of use; OA articles are governed by the applicable Creative Commons License

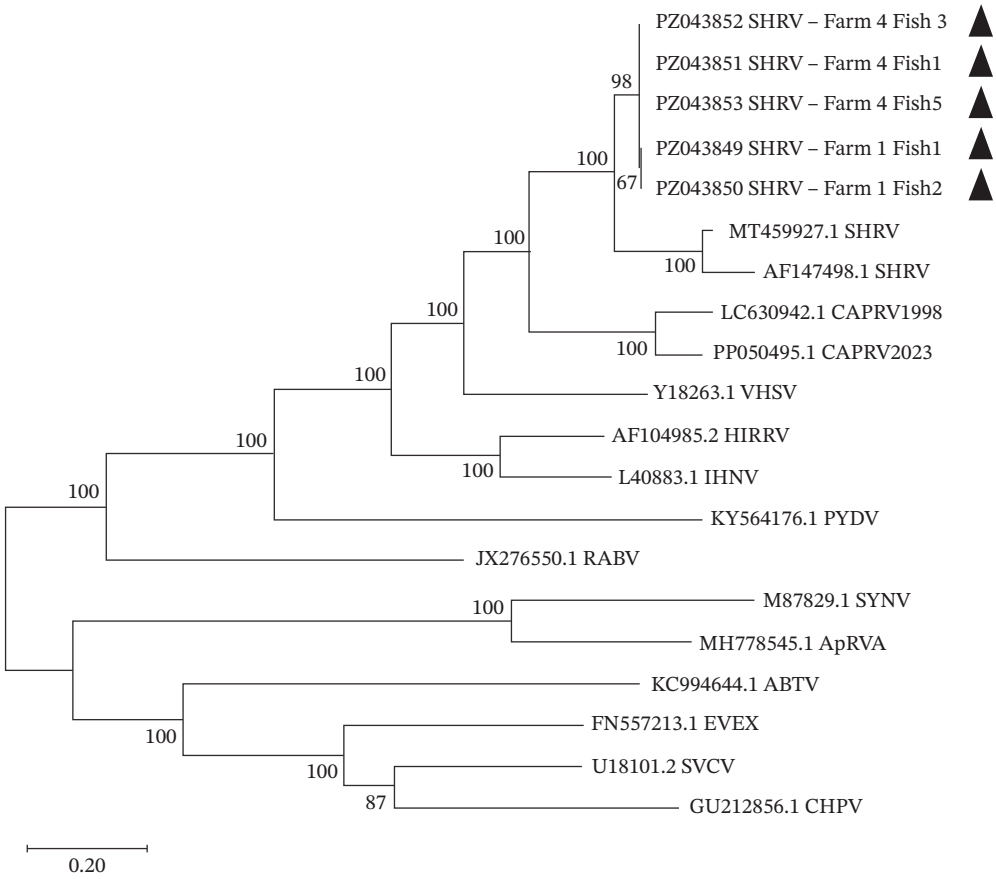

FIGURE 6 | Phylogenetic relationships of the SHRV-like *Novirhabdovirus* isolates KU-SHRV-CM01–05 (PZ043849–PZ043853) identified in giant snakehead (*C. micropeltes*) and representative members of the family Rhabdoviridae based on partial *L* gene sequences. The phylogenetic tree was reconstructed using the maximum likelihood method under the general time-reversible model with gamma-distributed rate variation among sites and a proportion of invariant sites (GTR + G + I). The tree with the highest log likelihood score is shown. Bootstrap support values ≥60%, calculated from 1000 replicates, are indicated at the corresponding nodes. The branch lengths represent the number of nucleotide substitutions per site. The analysis included 15 representative Rhabdoviridae reference sequences: snakehead rhabdovirus strain Thailand (SHRV; AF147498), SHRV strain India (MT459927), Carpione rhabdovirus strain Italy 1988 (CAPRV; LC630942), CAPRV strain China 2023 (CAPRV; PP050495), viral hemorrhagic septicemia virus (VHSV; Y18263), infectious hematopoietic necrosis virus (IHNV; L40883), Hirame rhabdovirus (HIRRV; AF104985), spring viremia of carp virus (SVCV; U18101), eel virus European X (EVEX; FN557213), Chandipura virus (CHPV; GU212856), rabies lyssavirus (RVPV, JX276550), Sonchus yellow net virus (SYNV; M87829), apple rootstock virus A (ApRVA, MH778545), potato yellow dwarf virus (PYDV; KY564176), and Arboretum virus isolate Lo-121 (ABTV, KC994644). The five sequences generated in this study (PZ043849–PZ043853) are indicated by triangles. Evolutionary analyses were performed using MEGA version 12.

SHRV but also raises concerns regarding disease surveillance and health management given the demand-driven shift to intensive giant snakehead production systems, where disease outbreaks have traditionally been attributed primarily to bacterial or parasitic etiologies [7–9].

The mortality events investigated in this study were characterized by rapid disease progression and cumulative mortality ranging from 7% to as high as 90% in some farms. These events were comparable to those reported in previous SHRV outbreaks among striped snakehead and hybrid species, which indicates that SHRV may be associated with severe diseases under intensive farming conditions [12, 14]. Although the affected farms were geographically separated across the central region of Thailand, that is, the provinces of Chachoengsao, Phetchaburi, and Bangkok, which are 80–180 km apart, all the farms obtained fry that had originally been sourced from the same natural reservoirs and had been stocked without prior health screening. In combination with routine exposure to untreated canal water and the use of raw forage fish as feed, these practices may have increased the likelihood of pathogen introduction and dissemination. While these factors cannot be confirmed as direct sources of infection, they highlight the possibility of biosecurity measures facilitating the emergence and spread of viruses in giant snakehead aquaculture.

Clinically, the moribund fish commonly exhibited signs consistent with epizootic ulcerative syndrome (EUS), including skin ulceration, fin erosion, lethargy, and abnormal swimming behavior [27]. EUS is recognized as a multifactorial condition in snakehead species and has been associated with a range of pathogens, such as fungi, bacteria, parasites, and viruses—particularly members of the family Rhabdoviridae [16, 28, 29]. In the present study, the highest mortality rates were observed in Farms 1 and 2, where SHRV occurred alongside *Aeromonas* spp. and *Trichodina* spp. The coinfected fish showed multifocal

tbed, 2026, 1, Downloaded from https://onlinelibrary.wiley.com/doi/10.1155/tbed/9677946 by University Of Stirling, Wiley Online Library on [10/08/2026]. See the Terms and Conditions (https://onlinelibrary.wiley.com/terms-and-conditions) on Wiley Online Library for rules of use; OA articles are governed by the applicable Creative Commons License

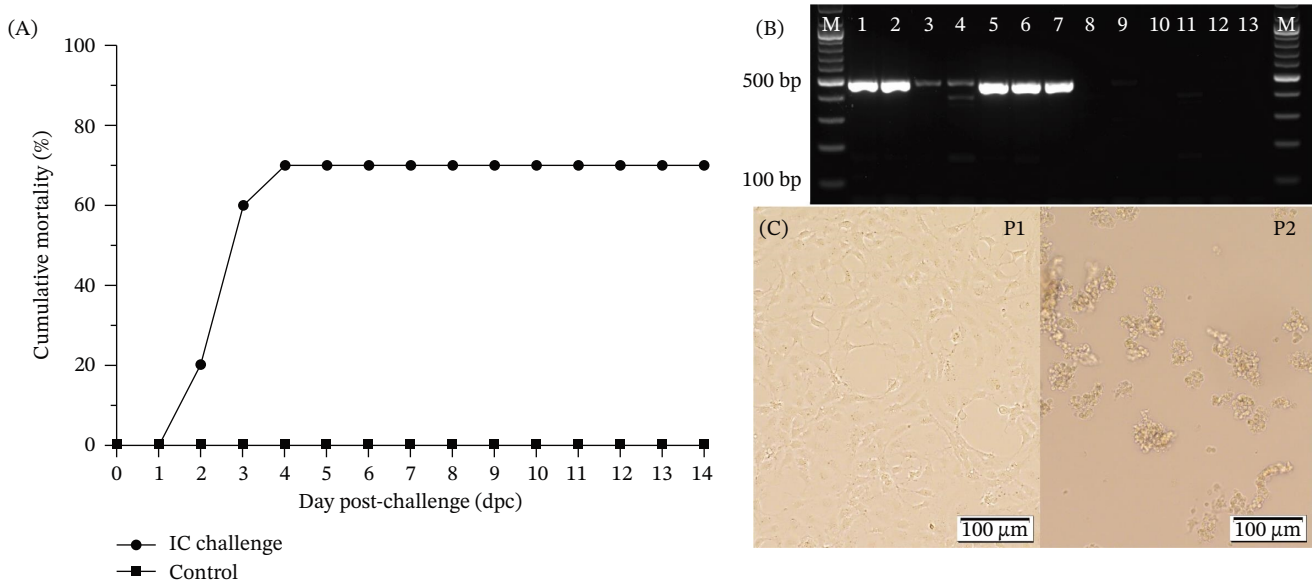

FIGURE 7 | Experimental challenge of naïve giant snakehead (*C. micropeltes*) with the SHRV-like *Novirhabdovirus* isolate KU-SHRV-CM03 for Koch's postulation. (A) Cumulative mortality over 14 days post-challenge (dpc) in fish ($n = 10$) intracelomic injected (IC challenge) with the SHRV-like *Novirhabdovirus* isolate KU-SHRV-CM03, and mock-challenged (control) fish ($n = 10$). (B) Detection of the rhabdovirus *L* gene (483 bp) by RT-PCR in posterior kidney samples collected from all experimentally challenged fish. Lane M, DNA molecular weight marker; Lane 1–2, moribund fish collected at 2 dpc; Lane 3–6, moribund fish collected at 3 dpc; Lane 7, moribund fish collected at 4 dpc; Lane 8–10, surviving challenged fish sampled at 14 dpc; Lane 11–12, control fish sampled at 14 dpc; Lane 13, no-template control. (C) CPE observed in E-11 cells following re-isolation of SHRV-like *Novirhabdovirus* from experimentally infected fish. First-passage (P1) cultures showed characteristic CPE affecting more than 50% of the cells within 2 dpi, while the second passage (P2) cultures demonstrated more rapid and extensive CPE, with widespread cell detachment and clumping observed by 2 dpi. Scale bar = 100 μm.

granulomatous inflammation in the liver, spleen, anterior kidney, and posterior kidney. Such lesions are commonly associated with bacterial infections in fish, including those caused by *Aeromonas* spp. [8] and are consistent with the bacteriological findings demonstrating concurrent bacterial infections in some farms included in this study. Therefore, some of the pathological changes observed in affected fish may have been influenced by concurrent infections in addition to SHRV infection, as previously reported in viral outbreaks involving secondary infections in teleost fish [30, 31]. Notably, SHRV was detected in fish from all eight farms investigated, including farms in which no bacterial or parasitic coinfections were identified. In particular, Farm 4 was negative for all screened bacterial and parasitic pathogens despite having substantial mortality, suggesting that the virus was associated with the observed disease outbreak. The detection of the virus was further supported by virus isolation from most RT-PCR-positive fish samples. Interestingly, one fish that tested negative by RT-PCR on the kidney tissue produced a positive virus isolation result in E-11 cells. This discrepancy may reflect a low viral burden in the original tissue sample, with subsequent viral replication in cell culture increasing the amount of detectable viral RNA. These findings emphasize the value of combining virus isolation with molecular assays when investigating an outbreak, particularly when establishing evidence for infection in a previously unreported host species. Additionally, the development of a quantitative PCR assay for SHRV would enable more accurate quantification of viral load and describe viral dynamics during infection.

Although our findings support a role of SHRV in these outbreaks, disease outcomes are likely influenced by multiple factors, including host condition, environmental stressors, viral load, and coinfecting pathogens [15, 25, 32–34]. Histopathological examination of SHRV-positive fish consistently revealed numerous eosinophilic ICIBs within the spleen, anterior kidney, and posterior kidney. These findings are indicative lesions of viral infection reported in other piscine *Novirhabdovirus* infections, including IHNV and VHSV [35, 36]. The lesions were accompanied by cellular degeneration, pyknotic nuclei, and the depletion of hematopoietic elements. Notably, one RT-PCR-negative fish showed ICIBs, which may be attributed to an unrelated cause of inclusion formation or discrepancy among the diagnostic assays. Together, these pathological changes suggest that the SHRV affects hematopoietic tissues and immune organs and may be associated with the anemia-like clinical signs observed in the giant snakehead. Damage to hematopoietic organs has also been reported in several viral diseases of teleost fish, including tilapia lake virus infection and infectious spleen and kidney necrosis virus infection, where necrosis and depletion of hematopoietic tissues were observed in the spleen and kidneys [37, 38]. As coinfections were detected in several farms, the lesions of fish collected from the farms and mortality observed in this study cannot be attributed solely to SHRV, and the relative contribution of SHRV and coinfecting pathogens to disease severity remains to be fully defined.

The isolation of SHRV in E-11 cells further demonstrated its infectivity and ability to replicate efficiently in fish cell cultures [39, 40]. Infected cells rapidly developed pronounced CPE within 1–2 dpi, and transmission electron microscopy revealed enveloped, bullet-shaped virions characterized as members of the

tbed, 2026, 1, Downloaded from https://onlinelibrary.wiley.com/doi/10.1155/tbed/9677946 by University Of Stirling, Wiley Online Library on [10/08/2026]. See the Terms and Conditions (https://onlinelibrary.wiley.com/terms-and-conditions) on Wiley Online Library for rules of use; OA articles are governed by the applicable Creative Commons License

family Rhabdoviridae [12, 15, 41]. In addition, the observation of virion budding from the plasma membrane indicated productive viral replication in E-11 cells, which is consistent with previous reports for other fish rhabdoviruses [12, 41, 42]. These findings support the suitability of E-11 cells for virus isolation and provide a useful platform for future investigations of viral replication and host–virus interactions. Importantly, experimental challenge with the isolated SHRV reproduced clinical disease consistent with those observed during the field outbreaks. The successful re-isolation of the virus from experimentally challenged fish provided evidence supporting the pathogenic role of SHRV in giant snakehead. Nevertheless, further studies using natural exposure routes, larger sample sizes, and defined infectious doses are required to elucidate the pathogenicity of SHRV in this species.

Phylogenetic analysis based on partial *L* gene sequence placed this SHRV detected in giant snakehead within the genus *Novirhabdovirus*, where they clustered with previously reported SHRV strains from striped snakehead in Thailand and India [12, 42]. Together with the CAPRV reference strains from Italy and China [43, 44], these formed a strongly supported SHRV–CAPRV cluster that was separated from other *Novirhabdoviruses* (VHSV, HIRRV, and IHNV). Although the observed *L* gene nucleotide divergence of 15%–20% between our isolates and previously reported SHRV strains indicates measurable sequence variation, the biology and taxonomic significance of this divergence cannot be determined from partial *L* gene data alone. Formal species classification within *Novirhabdovirus* relies primarily on glycoprotein (*G*) gene sequences and ideally requires whole-genome data and serological characterization [45]. Therefore, further complete genome characterization and phylogenetic analysis of multiple genes of this virus are still required for definitive species-level classification within the genus *Novirhabdovirus*.

5 | Conclusion

SHRV is an important viral pathogen of snakehead fish, and the present study provides the first evidence of an SHRV-like *Novirhabdovirus*-associated disease outbreaks in farmed giant snakehead in Thailand. The pathogenic role of the virus was supported by multiple complementary lines of evidence, including histopathological examination, RT-PCR detection and sequence analysis, virus isolation in susceptible cell lines, ultrastructural characterization by transmission electron microscopy, and experimental challenge followed by successful viral re-isolation, which fulfill the Koch's postulate. Phylogenetic analysis based on partial *L* gene sequences placed the SHRV from giant snakehead within the genus *Novirhabdovirus* and demonstrated their close genetic relationship with previously reported SHRV strains and CAPRV. However, definitive taxonomic classification of these isolates requires whole-genome characterization and comparative genomic analyses. Taken together, our findings highlight the importance of including SHRV-like *Novirhabdovirus* infection in the differential diagnosis of disease outbreaks in farmed giant snakehead and support its incorporation into routine disease surveillance programs. The results also emphasize the need for strengthened biosecurity practices, particularly with respect to fry sourcing, water management, and feeding strategies, to reduce the risk of pathogen introduction and disease transmission within aquaculture systems.

Author Contributions

Jidapa Yamkasem: conceptualization, data curation, investigation, methodology, validation, visualization, writing – original draft, writing – review and editing. **Natthakul Youngnoi**: conceptualization, investigation, methodology, visualization, writing – original draft. **Piyathip Setthawong**: methodology, validation, visualization. **Theeraporn Pulpipat**: conceptualization, methodology, validation. **Win Surachetpong**: conceptualization, writing – review and editing, supervision. **Tuchakorn Lertwanakarn**: conceptualization, data curation, validation, visualization, writing – original draft, writing – review and editing, project administration, funding acquisition, supervision.

Acknowledgments

The authors sincerely thank Supathida Meethong, S.O.R. Saha Pattana Inter Group Co., Ltd. and Mingbun Jitpaisarnvatana, Monkong Interfeed Co., Ltd. for their assistance in coordinating farm access and facilitating sample collection during the outbreak investigations. We are also grateful to Tharinee Limakom for her valuable support in field sampling and on-site data collection.

Funding

This research was financially supported by the Kasetsart University Research and Development Institute (KURDI) under the Project Number FF(KU) 56.69.

Disclosure

All authors have read and approved the final manuscript.

Ethics Statement

All animal handling and sampling procedures were approved by the Institutional Animal Care and Use Committee (IACUC) of Kasetsart University (Protocol Number ACKU68-VET-058). All procedures were conducted in accordance with institutional guidelines, and efforts were made to minimize animal stress and suffering.

Consent

The authors have nothing to report.

Conflicts of Interest

The authors declare no conflicts of interest.

Data Availability Statement

The nucleotide sequences generated in this study are openly available in the National Center for Biotechnology Information (NCBI) GenBank database (https://www.ncbi.nlm.nih.gov/) under Accession Numbers PZ043849–PZ043853.

References

1. S. Gao, D. Li, H. Hong, R. Shu, H. Cheng, and Y. Luo, "Comparison of Quality and Nutritional Attributes of Pond-Cultured and Container-Cultured Snakehead (*Channa argus argus*) Fillets After Being Boiled, Fried, and Baked," *Journal of Food Science* 85, no. 12 (2020): 4249–4259.

2. Z. Zeng, M. Zheng, M. Zhao, et al., "Comparison of Nutritional Value of Snakehead Fish From Guangdong and Deqing Varieties," *PLoS One* 19, no. 3 (2024): e0301203.

tbed, 2026, 1, Downloaded from https://onlinelibrary.wiley.com/doi/10.1155/tbed/9677946 by University Of Stirling, Wiley Online Library on [10/08/2026]. See the Terms and Conditions (https://onlinelibrary.wiley.com/terms-and-conditions) on Wiley Online Library for rules of use; OA articles are governed by the applicable Creative Commons License

3. W. Rojekittikhun, T. Chaiyasith, S. Nuamtanong, and C. Komalamisra, "Gnathostoma Infection in Fish Caught for Local Consumption in Nakhon Nayok Province, Thailand I. Prevalence and Fish Species," *The Southeast Asian Journal of Tropical Medicine and Public Health* 35, no. 3 (2004): 523–530.

4. L. X. Sinh, H. Navy, and R. S. Pomeroy, "Value Chain of Snakehead Fish in the Lower Mekong Basin of Cambodia and Vietnam," *Aquaculture Economics & Management* 18, no. 1 (2014): 76–96.

5. N. I. Ahmad, W. R. Wan Mahiyuddin, T. R. Tengku Mohamad, et al., "Fish Consumption Pattern Among Adults of Different Ethnics in Peninsular Malaysia," *Food & Nutrition Research* 60, no. 1 (2016): 32697.

6. R. Florance, E. Agusliani, and L. A. Sofia, "Development Strategy for Giant Snakehead Fish (*Channa micropeltes*) Production in South Barito Regency of Central Kalimantan," *Russian Journal of Agricultural and Socio-Economic Sciences* 138, no. 6 (2023): 183–187.

7. H. Novita, S. Andriyanto, D. Sugiani, et al., "Parasitic and Bacterial Diseases in Aquarium-Reared Indonesian Snakehead, (*Channa micropeltes*)," in *IOP Conference Series: Earth and Environmental Science*, 521, (IOP Publishing, 2020): 012019.

8. T. Pulpipat, T. I. Heckman, V. Boonyawiwat, et al., "Concurrent Infections of *Streptococcus iniae* and *Aeromonas veronii* in Farmed Giant Snakehead, (*Channa micropeltes*)," *Journal of Fish Diseases* 46, no. 6 (2023): 629–641.

9. E. A. Melchenkov, N. N. Romanova, A. P. Vorobyov, et al., "Ichthyopathological Examination of the Giant Snakehead (*Channa micropeltes* Cuvier, 1831)," *Rybovodstvo i rybnoe hozjajstvo (Fish Breeding and Fisheries)* (2025): 439–451.

10. World Organisation for Animal Health (WOAH), "Diseases Listed by WOAH [Internet]," 2024, [Cited 2025] https://www.woah.org/fileadmin/Home/eng/Health_standards/aahc/current/chapitre_diseases_listed.pdf.

11. W. Zeng, Q. Wang, Y. Wang, et al., "Isolation and Characterization of a Rhabdovirus From Snakehead Fish (*Ophicephalus striatus*)," *Journal of Fisheries of China* 37, no. 9 (2013): 1416.

12. K. R. John, M. R. George, P. Mageshkumar, et al., "Isolation and Characterisation of a Novel Rhabdovirus From Snakehead Fish Showing Surface Ulcerations and Mortality From India: First Report," *Aquaculture* 544 (2021): 737120.

13. H. Deng, S. Zheng, Y. Li, et al., "Isolation and Identification of Hybrid Snakehead Rhabdovirus (HSHRV) and Its Immune Response in the Hybrid Snakehead (Male *Channa argus* × Female *Channa maculata*)," *Microbial Pathogenesis* 196 (2024): 106983.

14. W. Ahne, P. E. V. Jørgensen, N. J. Olesen, and W. Wattanavijarn, "Serological Examination of a Rhabdovirus Isolated From Snakehead (*Ophicephalus striatus*) in Thailand With Ulcerative Syndrome," *Journal of Applied Ichthyology* 4, no. 4 (1988): 194–196.

15. P. E. Phelan, M. E. Pressley, P. E. Witten, M. T. Mellon, S. Blake, and C. H. Kim, "Characterization of Snakehead Rhabdovirus Infection in Zebrafish, (*Danio rerio*)," *Journal of Virology* 79, no. 3 (2005): 1842–1852.

16. K. R. John and M. R. George, "Viruses Associated With Epizootic Ulcerative Syndrome: An Update," *Indian Journal of Virology* 23, no. 2 (2012): 106–113.

17. World Organisation for Animal Health (WOAH), "Aquatic Animal Health Code [Internet]," 2019, [Cited 2025] https://rr-europe.woah.org/app/uploads/2020/08/oie-aqua-code_2019_en.pdf.

18. E. J. Emmenegger, T. R. Meyers, T. O. Burton, and G. Kurath, "Genetic Diversity and Epidemiology of Infectious Hematopoietic Necrosis Virus in Alaska," *Diseases of Aquatic Organisms* 40, no. 3 (2000): 163–176.

19. H. J. Kim, A. Cuenca, and N. J. Olesen, "Validation of a Novel One-Step Reverse Transcription Polymerase Chain Reaction Method for Detecting Viral Haemorrhagic Septicaemia Virus," *Aquaculture* 492 (2018): 170–183.

20. D. M. Stone, W. Ahne, K. L. Denham, et al., "Nucleotide Sequence Analysis of the Glycoprotein Gene of Putative Spring Viraemia of Carp Virus and Pike Fry Rhabdovirus Isolates Reveals Four Genogroups," *Diseases of Aquatic Organisms* 53, no. 3 (2003): 203–210.

21. D. F. Barreto-Vieira and O. M. Barth, "Negative and Positive Staining in Transmission Electron Microscopy for Virus Diagnosis," in *Microbiology in Agriculture and Human Health*, ed. M. M. Shah, (IntechOpen, 2015).

22. E. Bacharach, N. Mishra, T. Briese, et al., "Characterization of a Novel Orthomyxo-Like Virus Causing Mass Die-Offs of Tilapia," *mBio* 7, no. 2 (2016): e00431-16.

23. W. Liu, Y. Zhang, J. Ma, et al., "Determination of a Novel Parvovirus Pathogen Associated With Massive Mortality in Adult Tilapia," *PLOS Pathogens* 16, no. 9 (2020): e1008765.

24. Z. Yang, "Maximum Likelihood Phylogenetic Estimation From DNA Sequences With Variable Rates Over Sites: Approximate Methods," *Journal of Molecular Evolution* 39, no. 3 (1994): 306–314.

25. P. Michael, S. Panchavarnam, C. Bagthasingh, et al., "Innate Immune Response of Snakehead Fish to Indian Strain of Snakehead Rhabdovirus (SHRV-in) Infection and the Infectivity Potential of the Virus to Other Freshwater Fishes," *Fish & Shellfish Immunology* 149 (2024): 109577.

26. G. N. Frerichs, S. D. Millar, and R. J. Roberts, "Ulcerative Rhabdovirus in Fish in South-East Asia," *Nature* 322, no. 6076 (1986): 216.

27. World Organisation for Animal Health (WOAH), "Infection With *Aphanomyces invadans* (Epizootic Ulcerative Syndrome) [Internet]," 2023, [Cited 2023] https://www.woah.org/fileadmin/Home/eng/Health_standards/aahm/current/2.3.01_EUS.pdf.

28. G. N. Frerichs, "Viruses Associated With the Epizootic Ulcerative Syndrome (EUS) of Fish in South-East Asia," *Veterinary Research* 26, no. 5-6 (1995): 449–454.

29. R. K. Saylor, D. L. Miller, M. W. Vandersea, M. S. Bevelhimer, P. J. Schofield, and W. A. Bennett, "Epizootic Ulcerative Syndrome Caused by *Aphanomyces invadans* in Captive Bullseye Snakehead *Channa marulius* Collected From South Florida, USA," *Diseases of Aquatic Organisms* 88, no. 2 (2010): 169–175.

30. H. Ogut and N. Cavus, "A Comparison of Ectoparasite Prevalence and Occurrence of Viral Haemorrhagic Septicemia Virus (VHSV) in Whiting *Merlangius merlangus* Euxinus," *Revista de biología marina y oceanografía* 49, no. 1 (2014): 91–96.

31. P. Nicholson, N. Mon-on, P. Jaemwimol, P. Tattiyapong, and W. Surachetpong, "Coinfection of Tilapia Lake Virus and *Aeromonas hydrophila* Synergistically Increased Mortality and Worsened the Disease Severity in Tilapia (*Oreochromis* spp.)," *Aquaculture* 520 (2020): 734746.

32. G. N. Frerichs, "Stability of Snakehead (*Ophiocephalus striatus*) Rhabdovirus Under Different Environmental Conditions," *Journal of Applied Ichthyology* 5, no. 3 (2008): 122–126.

33. M. K. Purcell, K. J. Laing, and J. R. Winton, "Immunity to Fish Rhabdoviruses," *Viruses* 4, no. 1 (2012): 140–166.

34. K. M. Lee, D. H. Kim, and K. H. Kim, "Replication of Heterologous Glycoprotein-Expressing Chimeric Recombinant Snakehead Rhabdoviruses (rSHRVs) and Viral Hemorrhagic Septicemia Viruses (rVHSVs) at Different Temperatures," *Virus Research* 297 (2021): 198392.

35. T. Isshiki, T. Nishizawa, T. Kobayashi, T. Nagano, and T. Miyazaki, "An Outbreak of VHSV (viral Hemorrhagic Septicemia Virus) Infection in Farmed Japanese Flounder *Paralichthys olivaceus* in Japan," *Diseases of Aquatic Organisms* 47, no. 2 (2001): 87–99.

36. S. Ahmadivand, M. Soltani, K. Mardani, et al., "Infectious Hematopoietic Necrosis Virus (IHNV) Outbreak in Farmed Rainbow Trout in Iran: Viral Isolation, Pathological Findings, Molecular Confirmation, and Genetic Analysis," *Virus Research* 229 (2017): 17–23.

tbed, 2026, 1, Downloaded from https://onlinelibrary.wiley.com/doi/10.1155/tbed/9677946 by University Of Stirling, Wiley Online Library on [10/08/2026]. See the Terms and Conditions (https://onlinelibrary.wiley.com/terms-and-conditions) on Wiley Online Library for rules of use; OA articles are governed by the applicable Creative Commons License

37. Z. Zhu, C. Duan, Y. Li, et al., "Pathogenicity and Histopathology of Infectious Spleen and Kidney Necrosis Virus Genotype II (ISKNV-II) Recovering From Mass Mortality of Farmed Asian Seabass, *Lates calcarifer*, in Southern China," *Aquaculture* 534 (2021): 736326.

38. N. Youngnoi, J. Yamkasem, M. Khemthong, et al., "Granulocyte Tropism and Lymphocyte Depletion Highlight the Immunopathogenesis of Tilapia Lake Virus Infection in Nile Tilapia," *Fish & Shellfish Immunology* 163 (2025): 110410.

39. J.-R. Hong, T.-L. Lin, Y.-L. Hsu, and J.-L. Wu, "Apoptosis Precedes Necrosis of Fish Cell Line With Infectious Pancreatic Necrosis Virus Infection," *Virology* 250, no. 1 (1998): 76–84.

40. A. F. Pearce and D. S. Lyles, "Vesicular Stomatitis Virus Induces Apoptosis Primarily Through Bak Rather Than Bax by Inactivating Mcl-1 and Bcl-XL," *Journal of Virology* 83, no. 18 (2009): 9102–9112.

41. G. D. Lio-Po, G. S. Traxler, L. J. Albright, and E. M. Leaño, "Characterization of a Virus Obtained From Snakeheads *Ophicephalus striatus* With Epizootic Ulcerative Syndrome (EUS) in the Philippines," *Diseases of Aquatic Organisms* 43 (2000): 191–198.

42. J. Kasornchandra, H. M. Engelking, C. N. Lannan, J. S. Rohovec, and J. L. Fryer, "Characteristics of Three Rhabdoviruses From Snake-Head Fish, *Ophicephalus striatus*," *Diseases of Aquatic Organisms* 13 (1992): 89–94.

43. G. Bovo, N. J. Olesen, P. E. V. Jørgensen, W. Ahne, and J. R. Winton, "Characterization of a Rhabdovirus Isolated From Carpione *Salmo trutta carpio* in Italy," *Diseases of Aquatic Organisms* 21 (1995): 115–122.

44. H. Sun, J. Huang, H. Wang, et al., "Mass Mortality Associated With Carpione Rhabdovirus in Golden Pompano (*Trachinotus ovatus*) in China: First Report," *Aquaculture* 595 (2025): 741638.

45. International Committee on Taxonomy of Viruses, *Genus: Novirhabdovirus. ICTV Virus Taxonomy: 10th Report on the Taxonomy of Viruses (Online)*, 2023, Rhabdoviridae Chapter https://ictv.global/report/chapter/rhabdoviridae/rhabdoviridae/novirhabdovirus.

Supporting Information

Additional supporting information can be found online in the Supporting Information section. **Supporting Information 1**. Table S1: Summary of SHRV detection by RT-PCR, parasitic and bacterial coinfections, and histopathological findings in giant snakehead collected from eight farms during disease outbreak investigations in Thailand from January to April 2025. **Supporting Information 2**. Figure S1: Histopathological findings in other organs of the moribund giant snakehead from Farm 4. (A) Gills show lamellar edema (black arrows) and mild lymphocytic infiltration (arrowheads). (B) Brain exhibits mild vascular congestion (asterisks). (C) Intestinal tissue shows no remarkable histopathological alterations. (D) Heart demonstrates normal myocardial architecture without significant lesions.

tbed, 2026, 1, Downloaded from https://onlinelibrary.wiley.com/doi/10.1155/tbed/9677946 by University Of Stirling, Wiley Online Library on [10/08/2026]. See the Terms and Conditions (https://onlinelibrary.wiley.com/terms-and-conditions) on Wiley Online Library for rules of use; OA articles are governed by the applicable Creative Commons License